# Dissipation by transfer and its influence on fusion

*Giulia* Colucci[1,*], *Agnieszka* Trzcińska[1,**], *Pei Wei* Wen[2], and *Ernest* Piasecki[1]

[1]Heavy Ion Laboratory, University of Warsaw, Warszawa, Poland
[2]China Institute of Atomic Energy, Beijing, China

**Abstract.** A new version of the CCQEL code has been developed by upgrading the method of coupling of transfer channels during fusion and backscattering processes. In particular, the number of transfer reactions included has been increased and the dependence of the strength of transfer coupling on the transferred particle and experimental Q-value distribution was introduced. The upgraded code was employed for the investigation of the influence of transfer on the smoothing of the measured quasielastic barrier distribution ($D_{qe}$) of the $^{24}$Mg + $^{92}$Zr and $^{20}$Ne + $^{208}$Pb systems and found interesting discrepancies with respect to the standard approximations. The study with the upgraded code indicates the transfer responsible for generating strongly excited targets as the leading cause of the smearing of the barrier distribution, even in the case of negative ground state to ground state Q value ($Q_{gg}$). The smoothing observed in the barrier distribution is dominated rather by one neutron transfer, despite the negative $Q_{gg}$ value for this reaction and the positive $Q_{gg}$ value for two-neutron transfer. Of particular interest is the case of the $^{20}$Ne + $^{208}$Pb, where the smoothing of the $D_{qe}$ is mainly influenced by the one neutron pick-up at the beam energy above the barrier, while the one neutron pick-up and one proton stripping transfers are dominant for lower beam energy. These results highlight the importance of the transfer coupling dependence on the experimental Q-value distribution and, consequently, on the projectile kinetic energy.

## 1 Introduction

The Coupled Channels (CC) method successfully addressed the study of the influence of a small number of projectile and target collective excitations on near- and sub-barrier fusion [1, 2]. As a result of the couplings of the relative motion to intrinsic degrees of freedom, the barrier splits into several distributed barriers, giving a fingerprint of the structure of the interacting nuclei and the dynamics of the reaction.

Although the CC model well established the role of couplings to collective excitations on the barrier distributions for many systems [3], there are still mechanisms whose impact on fusion is less understood. Among these is dissipation, where the kinetic energy of the relative motion between the projectile and target is partially dissipated into the internal degrees of freedom of the interacting nuclei. Consequently, the experimental barrier distributions of some systems get distorted, or the structure gets completely blurred in comparison with theoretical CC predictions [4–6].

Two mechanisms are mainly responsible for dissipation: excitation of non-collective levels by nuclear and electromagnetic interactions [7–9] and mutual projectile-target transfer of light particles. The first one has been treated by the CCRMT model, which combines the CC method with the Random Matrix Theory (RMT), with promising results [6, 9]. The influence of transfer was both experimentally and theoretically investigated. However, the conclusions are still contradictory because of the complicated nature of this many-body time-dependent phenomenon. In this framework, the study of the $^{24}$Mg + $^{92}$Zr and $^{20}$Ne + $^{208}$Pb systems is particularly interesting.

The quasielastic barrier distribution of the $^{24}$Mg + $^{92}$Zr was measured and compared to the $^{24}$Mg + $^{90}$Zr system [6]. According to the standard CC calculations, the strong deformation of the $^{24}$Mg projectile should result in the domination of the projectile in the determination of the $D_{qe}$, giving rise to very similar structured shapes of barrier distributions for both systems. Contrary to theoretical expectations, the barrier distribution structure was visible in the $^{90}$Zr, while it was washed out for the $^{92}$Zr isotope. Calculations using the CC+RMT model qualitatively supported this observation, identifying the partial energy dissipation caused by the coupling of relative motion of the projectile and target nuclei to many single-particle excitations, as an explanation of the smoothed structure in the $^{24}$Mg + $^{92}$Zr case. However, the theoretical barrier distributions were visibly narrower in comparison with the experimental ones (see Fig. 8 of [6]). One hypothesis for this disagreement was proposed being the coupling to transfer channels.

Different is the case of the $^{20}$Ne + $^{208}$Pb system. The measurement of the quasielastic barrier distribution for the $^{20}$Ne + $^{208}$Pb system [10] found a single broad structureless peak, in marked contrast to the results of coupled-channels calculations, including couplings to the strongest collective states in both projectile and target,

*e-mail: colucci@slcj.uw.edu.pl
**e-mail: agniecha@slcj.uw.edu.pl

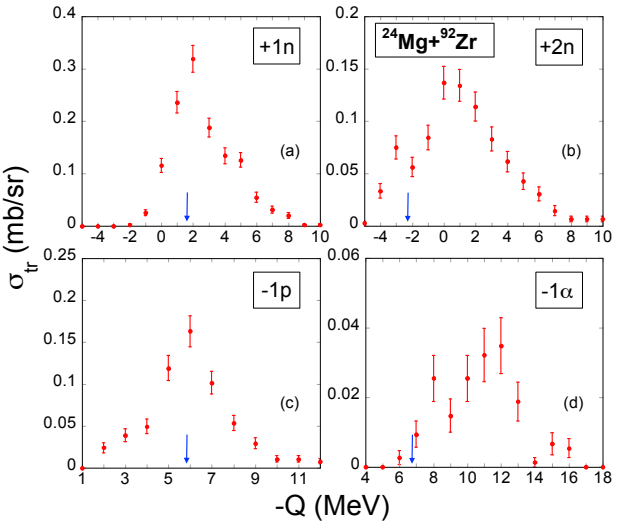


**Figure 1.** Q-value distributions expressed in 1MeV binning for the strongest transfer channels of the $^{24}$Mg + $^{92}$Zr system. The blue arrows indicate the $Q_{gg}$ value for each transfer channel.

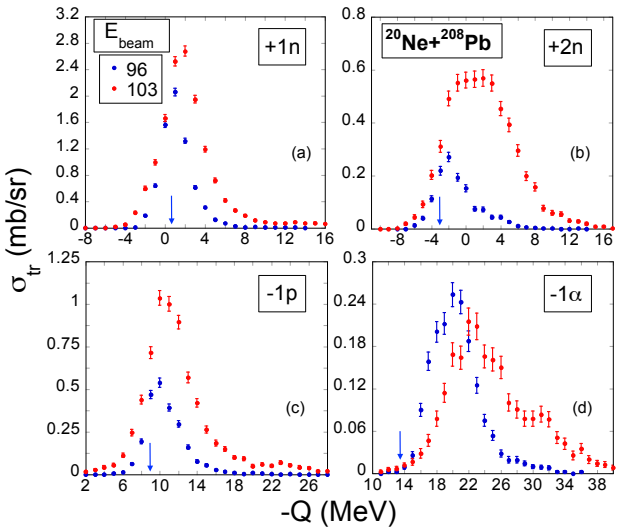


**Figure 2.** Q-value distributions expressed in 1MeV binning for the strongest transfer channels of the $^{20}$Ne + $^{208}$Pb system at the beam energies of 96 MeV and 103 MeV. The blue arrows indicate the $Q_{gg}$ value for each transfer channel.

which showed a pronounced double-peaked structure. However, as a doubly magic nucleus, $^{208}$Pb has a much lower density of non-collective states; therefore, the calculations, taking them into account, can only slightly smooth the barrier distribution [4]. This suggests that another mechanism is responsible for the barrier smoothing in the $^{20}$Ne + $^{208}$Pb system.

## 2 Results

Recently we modified the code CCQEL [11], upgrading the method of coupling of transfer channels during fusion and backscattering processes. The standard CCQEL code can include the two-neutron transfer channels, treated as pair-transfer coupling between the ground states. Under this condition, the transfer coupling form factor is expressed as:

$$F_{tr} * \frac{dV_n}{dr}, \qquad (1)$$

where $V_n$ is the nuclear potential [12, 13]. The coefficient $F_{tr}$ is the coupling strength, and according to this model, it is independent of:

- the type of the transferred light particle(s);
- the reaction's Q-value (usually g.s. to g.s. transfer ($Q_{gg}$) is assumed, independently of the projectile energy).

Moreover, since the two neutrons transfer with positive $Q_{gg}$ is frequently assumed dominant, one usually considers only this kind of transfer. The transfer coupling strength $F_{tr}$ is usually fitted in the range of 0.0 - 0.5 fm [14–16] to reach an agreement between the experimental and theoretical excitation functions.

We measured the Q-value distributions for various transfer channels in the backscattering of the $^{24}$Mg + $^{92}$Zr [17] and $^{20}$Ne + $^{208}$Pb [18] systems. The Q-distributions for the one and two neutron pick-up and one proton and alpha stripping channels for the $^{24}$Mg + $^{92}$Zr and $^{20}$Ne + $^{208}$Pb [18] systems are shown in Fig. 1 and 2, respectively. In the case of $^{20}$Ne + $^{208}$Pb, the measurements were performed at two beam energies. Measurements of the Q-value distribution for transfers at near-barrier energies almost always have a significant part above the $Q_{gg}$ value, corresponding to negative excitation energy E$^*$ [19, 20]. This non-physical effect was also observed in our measurements and results from the experimental energy resolution. Thus, to exploit the information from the Q distributions, we performed the deconvolution of experi-

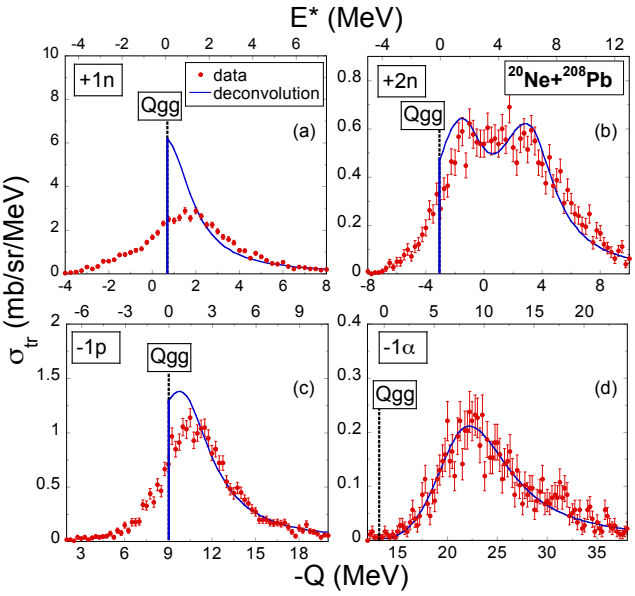


**Figure 3.** Examples of deconvolution of the Q-value distributions for the four dominant transfers of the $^{20}$Ne + $^{208}$Pb system at the beam energy of 103 MeV. The experimental Q-distributions are shown employing the bin's width of 0.25 MeV.

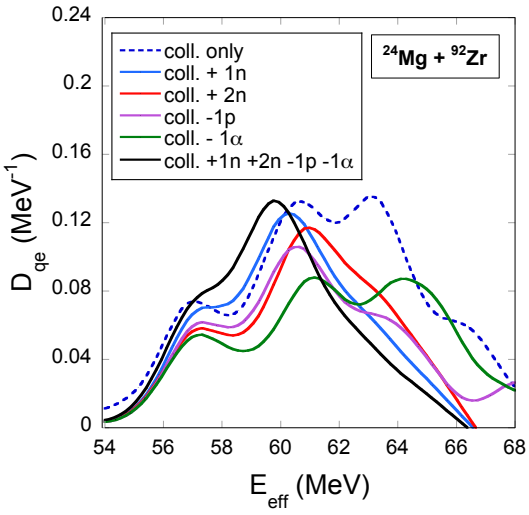


**Figure 4.** Quasielastic barrier distributions for the $^{24}$Mg + $^{90,92}$Zr system calculated with the improved CCQEL code. The calculations were performed taking into account simultaneously (black solid line) and separately the four main transfer channels: 1 neutron pick-up (blue solid line), 2 neutron pick-up (red solid line), 1 proton stripping (purple solid line) and 1alpha stripping (green solid line). The results are compared with the CC calculations which only consider collective excitations (blue dashed line).

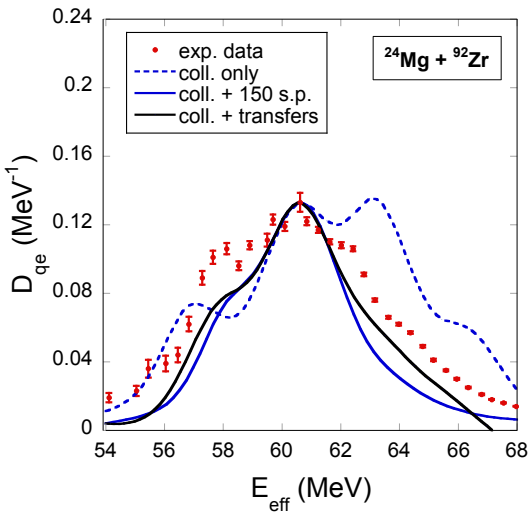


**Figure 5.** Comparison of the experimental quasielastic barrier distributions for the $^{24}$Mg + $^{90,92}$Zr system (red solid circles) with the theoretical CC calculations obtained including only the collective excitations (blue dashed line), the coupling of collective and non-collective excitations (blue solid line) and the couplings of the collective excitations to the four main transfer channels (black solid line). The latter theoretical curve was shifted to higher energy by 0.78 MeV to compare the $D_{qe}$ structures. For the calculated barrier distributions, the experimental resolution of 0.6 MeV (FWHM) was taken into account. All theoretical curves are normalized at the peak of the experimental data.

mental Q-value distributions, considering the cut-off at the $Q_{gg}$, i.e., at $E^* = 0$. The results of the deconvolution procedure for the $^{20}$Ne + $^{208}$Pb at the beam energy of 103 MeV are shown in Fig. 3.

The information from the deconvoluted Q-distributions is used in the upgraded CCQEL code. More in detail, the modified CCQEL code used in this work allows to:

- specify the mass and atomic numbers of the transfer particles;
- include simultaneously various transfer channels;
- perform simultaneous calculations with various Q and $F_{tr}(Q)$ values determined from the experimental Q-value distributions.

Comparing the experimental transfer cross section corresponding to the Q-values to the calculated ones provides us with the $F_{tr}(Q)$ values. This procedure is performed for each transfer channel of interest.

### 2.1 The case of $^{24}$Mg + $^{92}$Zr

The transfer cross sections for systems $^{24}$Mg + $^{90,92}$Zr at near barrier energy 76 MeV at the backward angle 142 degrees were measured and preliminary results were presented in [17].

The differential transfer cross section for the $^{92}$Zr resulted significantly bigger than the $^{90}$Zr one [17]. The measurement indicates the single-neutron pickup as the dominant transfer reaction, but the single-proton stripping and two-neutron pick-up are of comparable importance. The alpha stripping channel is present but significantly weaker than the abovementioned transfers.

The ion-ion potential used in the calculation was of the Woods-Saxon shape. The Akyüz-Winther potential parameters were $V_0 = 64.8$ MeV, $r_0 = 1.18$ fm and $a = 0.65$ fm for the real part, and $W_0 = 30$ MeV, $r_{0W} = 0.9$ fm and $a_W = 0.5$ fm for the imaginary part. The vibrational couplings to the first $2^+$ state at 0.93 MeV and the first $3^-$ state at 2.34 MeV in $^{92}$Zr were included. The deformation parameters of $\beta_2 = 0.1$ and $\beta_3 = 0.17$ [21, 22] were used. The couplings between the $0^+$, $2^+$, $4^+$, and $6^+$ states in the $^{24}$Mg rotational band were also included. The deformation parameters were $\beta_2 = 0.59$ and $\beta_4 = -0.03$ [23].

Employing the upgraded CCQEL code, the collective excitations of target and projectile nuclei were coupled to the four main transfer channels (one and two neutron pick-up, one proton and alpha stripping) of the $^{24}$Mg + $^{90,92}$Zr reaction. The coupling strength factors $F_{tr}(Q)$ were adjusted to provide a good agreement between the theoretical and experimental Q-distributions. Figure 4 shows the influence of each transfer channel on the structure of the quasielastic barrier distributions. According to the calculations, the single neutron pick-up seems to be the dominant channel. Indeed, the coupling to the +1n transfer (blue solid curve in Fig. 4) considerably smooths out the $D_{qe}$ structure generated by collective excitations similarly to the $D_{qe}$ obtained including all four transfer reactions simultaneously (black solid curve in Fig. 4). The results are shown in Fig. 5 in comparison to the experimental $D_{qe}$. The calculations show that, according to the model, transfers can significantly change the barrier distribution shape,

smoothing out the structure (a few peaks) resulting from the collective excitations (dashed blue curve in Fig. 5). The calculations obtained including the non-collective excitations, e.g. 150 single-particle (s.p.) levels, (blue solid curve in Fig. 5) smooth out the $D_{qe}$ structure, similarly to the result achieved considering the transfers. This suggests the necessity of integrating the dissipation due to simultaneous non-collective excitations and transfer reactions to reproduce the experimental barrier distribution.

### 2.2 The case of $^{20}$Ne + $^{208}$Pb

The transfer reaction cross sections at a backward angle and two incident energies corresponding to the calculated (but not observed) structure in $D_{qe}$ for the $^{20}$Ne + $^{208}$Pb system were measured [18]. In terms of the differential transfer cross section, the essential reaction turned out to be the single-neutron pickup and the single-proton stripping, while the two-neutron pick-up is of comparable importance to the single-proton stripping. The alpha stripping was also significant.

Dissimilarly to the $^{24}$Mg + $^{90,92}$Zr case, where the transfer cross sections were measured at one near barrier energy, for $^{20}$Ne + $^{208}$Pb, the measurements were made at two beam energies at 96 MeV and 103 MeV. This allow us to check the dependence of the $F_{tr}$ parameter on the projectile's kinetic energy.

A Woods-Saxon-shaped ion-ion potential was employed in the calculations. The Akyüz-Winther potential parameters were $V_0$ = 69.3 MeV, $r_0$ = 1.18 fm and $a$ = 0.66 fm for the real part, and $W_0$ = 30 MeV, $r_{0W}$ = 0.9 fm and $a_W$ = 0.5 fm for the imaginary part. For collective excitations, we have included couplings to the first $3^-$ state at 2.614 MeV and the first $2^+$ state at 4.07 MeV in $^{208}$Pb within the two and one phonons vibrational coupling scheme, respectively. The deformation parameters of $\beta_3 = 0.11$ and $\beta_2 = 0.055$ [21, 24] were used. The calculations also included the couplings between the $0^+$, $2^+$, $4^+$, and $6^+$ states in the $^{20}$Ne rotational band. The large deformation parameters for $^{20}$Ne, $\beta_2 = 0.46$ and $\beta_4 = 0.27$ [25] were employed.

In addition to the collective excitations of projectile and target nuclei, the main transfer channels were taken into account, where the corresponding $F_{tr}$(Q) values were adjusted to minimize the difference between the calculated and deconvoluted experimental Q-value distributions. Figure 6 compares the quasielastic barrier distributions obtained by gradually including the four strongest transfer reactions starting from the one neutron pick-up. Because of the two beam energy measurements, the comparison is performed for the $F_{tr}$ obtained separately at 103 MeV and 96 MeV (panels (a) and (b) of Fig. 6, respectively). At beam energies above the barrier, the influence of one neutron pick-up seems to dominate: the couplings to the +1n transfer lead to a significant smoothing of the two peaks structure of the barrier distributions, while the other transfer channels only slightly influence the structure established by the one neutron pick-up. A different situation appears at energies below the barrier, where the one neutron pick-up and one proton stripping strongly modify the

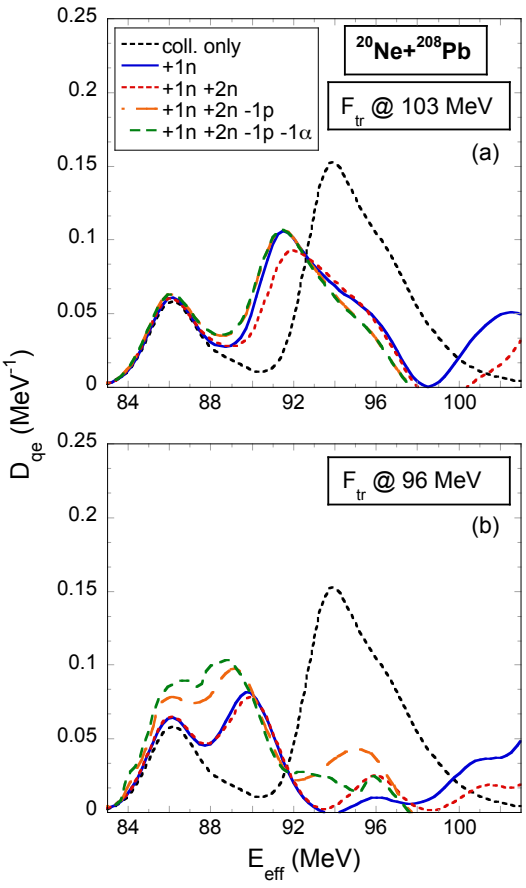


**Figure 6.** Comparison of the quasielastic barrier distributions of the $^{20}$Ne + $^{208}$Pb system obtained within the upgraded CCQEL code including only the collective excitations (dashed black line) and by gradually including the four strongest transfer reactions starting from the one neutron pick-up: +1n transfer (blue solid line), +1n and +2n transfers (red dashed line), +1n +2n and -1p transfers (orange dashed line) and +1n + 2n -1p and -1$\alpha$ transfers (green dashed line). The $F_{tr}$(Q) values were obtained from the experimental Q distributions measured at the beam energies of 103 MeV (a) and 96 MeV (b).

structure of the barrier distributions by considerably narrowing it.

A comparison of calculations with the experimental data is shown in Fig. 7. The coupling to states with large excitation energy leads to the adiabatic potential renormalization, consisting of an energy-independent potential shift [3]. Since this mainly affects the height of the Coulomb barrier, without influencing the shape of the barrier distributions, we shifted the calculated barrier distributions by 3.7 MeV to overlap with experimental data. The coupling to the four transfer reactions leads to smoother barrier distributions. However, the calculations are still not able to reproduce the experimental data. Furthermore, the comparison of quasielastic barrier distributions obtained for the two sets of $F_{tr}$ (blue and red solid curves of Fig. 7) highlights the barrier distributions' strong beam energy dependence. This is a direct consequence of the beam energy dependence of the Q distributions, presented in Fig. 2. Including the $F_{tr}$ beam energy dependence would probably

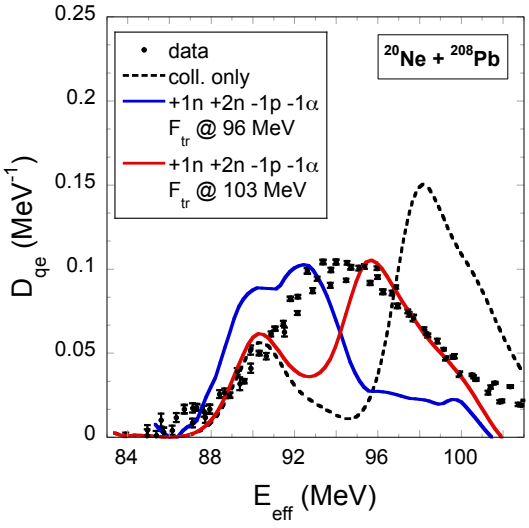


**Figure 7.** Comparison of the quasielastic barrier distribution for the $^{20}$Ne + $^{208}$Pb system with the CC calculations performed with only the collective excitations (dashed black line) and the four strongest transfer channels. The $F_{tr}$(Q) values were obtained from the Q distribution measurements performed at the beam energy of 96 MeV (blue solid line) and 103 MeV (red solid line). For the calculated barrier distributions, the experimental resolution of 0.7 MeV (FWHM) was taken into account. The theoretical curves were shifted to higher energy by 3.7 MeV.

lead to stronger smoothing and broader barrier distributions, as observed experimentally.

## 3 Summary and Conclusions

An upgraded CCQEL code was developed and employed to investigate the influence of the dissipation due to transfer reactions on the smoothing of the measured quasielastic barrier distribution of the $^{24}$Mg + $^{92}$Zr and $^{20}$Ne + $^{208}$Pb systems. The results found interesting discrepancies with respect to the standard approximations. The transfers responsible for generating strongly excited targets are the leading cause of the smearing of the barrier distribution. Furthermore, the two neutrons transfer, even having a positive $Q_{gg}$ value (+2.59 MeV and +3.03 MeV for the $^{24}$Mg + $^{92}$Zr and $^{20}$Ne + $^{208}$Pb, respectively) is not necessarily dominating. Indeed, the smoothing observed in the barrier distribution $D_{qe}$ is led by one neutron transfer, despite the negative $Q_{gg}$ value for this reaction and the positive $Q_{gg}$ for two neutrons transfer.

Concerning the $^{24}$Mg + $^{92}$Zr system, the quasielastic barrier distributions calculated including the non-collective excitations, within the CCRMT model, and taking into account the four main transfer channels similarly smooth out the structure generated by the collective excitations. However both $D_{qe}$ are still narrower in comparison to the experimental one. This suggests that it is the dissipation due to the combination of the excitation of single-particle levels and transfer reactions responsible for the smoothing of the experimental $D_{qe}$ of $^{24}$Mg + $^{92}$Zr system. Unfortunately, at the moment there is no available code able to take into account together non-collective excitations and transfers.

The availability of transfer cross-section measurements performed at two beam energies, in the case of $^{20}$Ne + $^{208}$Pb, allowed us to investigate the influence of the transfer channels on $D_{qe}$ according to the projectile's kinetic energy. In particular, two different sets of coupling strength parameters $F_{tr}$ were obtained for each transfer reaction. For the higher beam energy, the smoothing of the barrier distribution is dominated not by 2n but rather by 1n pick-up. On the other hand, for the lower beam energy, additionally to the 1n pick-up, the smoothing is dominated by the 1p stripping channel. Generally, the coupling to the four transfer reactions generates smoother barrier distributions. However, a satisfactory agreement with the experimental data has not been reached. Furthermore, a strong beam energy dependence is observed because of the significantly different shapes of $D_{qe}$ obtained for the two sets of $F_{tr}$. This is a direct consequence of the beam energy dependence of the Q-distributions. Including of the $F_{tr}$ beam energy dependence in the model should probably lead to the stronger smoothing observed experimentally.

## Acknowledgements

We are grateful to Prof. Hagino for his availability and fruitful discussions. This work was partly funded by the SHENG1 project under contract No. 2018/30/Q/ST2/00163 and the IDUB project under the contract No. PSP 501-D355-20-0002220. The work of P.W.W. is supported by the National Natural Science Foundation of China (Grants No. 12375130), and the Director's Foundation of Department of Nuclear Physics, China Institute of Atomic Energy (12SZJJ-202305).

## References

[1] M. Dasgupta, D. J. Hinde, N. Rowley, and A. M. Stefanini, Annu. Rev. Nucl. Part. Sci. **48**, 401 (1998)
[2] B. B. Back, H. Esbensen, C. L. Jiang, and K. E. Rehm, Rev. Mod. Phys. **86**, 317 (2014)
[3] K. Hagino and N. Takigawa, Prog. Theo. Phys. **128**, 1061 (2012)
[4] E. Piasecki et al., Phys. Rev. C **80**, 054613 (2009)
[5] A. Trzcińska et al., Phys. Rev. C **92**, 034619 (2015)
[6] A. Trzcińska et al., Phys. Rev. C **102**, 034617 (2020)
[7] S. Yusa, K. Hagino, and N. Rowley, Phys. Rev C **82**, 024606 (2010).
[8] S. Yusa, K. Hagino, and N. Rowley, Phys. Rev. C **88**, 054621 (2013)
[9] E. Piasecki, M. Kowalczyk, S. Yusa, A. Trzcińska, and K. Hagino, Phys. Rev. C **100**, 014616 (2019)
[10] E. Piasecki at al., Phys. Rev. C **85**, 054608 (2012)
[11] K. Hagino, N. Rowley, and A. T. Kruppa, Comput. Phys. Commun. **123**, 143 (1999)
[12] C. Dasso and G. Pollarolo, Physics Letters B**155**, 223 (1985)
[13] C. Dasso and A. Vitturi, Physics Letters B **179**, 337 (1986)

[14] N. K. Deb et al., Phys. Rev. C **102**, 034603 (2020)
[15] A. M. Stefanini et al., Phys. Rev. C **96**, 014603 (2017)
[16] R. N. Sahoo et al., Phys. Rev. C **102**, 024615 (2020)
[17] D. Wójcik et al., Acta Phys. Pol. B **49**, 387 (2018)
[18] E. Piasecki et al., Phys. Rev. C **85**, 054604 (2012)
[19] T. Mijatović et al., Phys. Rev. C **94**, 064616 (2016)
[20] J. Diklić et al., Phys. Rev. C **107**, 014619 (2023)
[21] S. Raman, At. Data and Nucl. Data Tabl. **78**, 1 (2001)
[22] R. H. Spear, At. Data Nucl. Data Tables **42**, 55 (1998)
[23] G. S. Blanpied et al., Phys. Rev. C **25**, 422 (1982)
[24] T. Kibedi and R. H.Spear, At. Data Nucl. Data Tables **80**, 35 (2002)
[25] G. S. Blanpied et al., Phys. Rev. C **38**, 2180 (1988)